Hyperbaric Oxygen Promotes Chronic Wound Healing in Sprague-Dawley Rats by Inhibiting Pyroptosis

Huadan MA[1,2], Xi WEI[3], Erbing LIN[4], Yingchuan WANG[4], Junjie HUANG[5], Hua WEI[5]

[1]Department of Hyperbaric Oxygen, Affiliated Hospital of Youjiang Medical University for Nationalities, Baise, Guangxi, China, [2]Guangxi Clinical Medical Research Center for Hepatobiliary Diseases, Baise, Guangxi, China, [3]Health supervision center, Affiliated Hospital of Youjiang Medical University for Nationalities, Baise, Guangxi, China, [4]Department of General Medicine, Affiliated Hospital of Youjiang Medical University for Nationalities, Baise, Guangxi, China, [5]School of Basic Medical Science, Youjiang Medical University for Nationalities, Baise, Guangxi, China

Received May 6, 2024
Accepted July 9, 2024

Summary

This study aimed to establish a rat model of chronic wounds to observe the effects of hyperbaric oxygen (HBO) on chronic wound repair and pyroptosis and explore the potential role of pyroptosis in the pathogenesis of chronic wounds. Sprague-Dawley (SD) rats were randomly divided into acute wound group (control group), chronic wound group (model group), chronic wound + HBO treatment group (HBO group), and chronic wound + VX-765 (IL-converting enzyme/Caspase-1 inhibitor) treatment group (VX-765 group). After 7 days of respective interventions, the wound healing status was observed, and wound tissue specimens were collected. Hematoxylin and eosin (HE) staining was used to observe the pathological changes in wound tissues. Transmission electron microscopy was used to observe the changes in cellular ultrastructure. Immunofluorescence was used to observe the expression and localization of vascular endothelial growth factor A (VEGF-A) and the N-terminal domain of gasdermin D (GSDMD-N). Western blot was conducted to detect the expression of nucleotide-binding oligomerization domain-like receptor protein 3 (NLRP3), cysteine-requiring aspartate protease-1 (Caspase-1), VEGF-A, and GSDMD-N proteins in wound tissues. Real-time quantitative reverse transcription polymerase chain reaction (qRT-PCR) was used to detect the expression of NLRP3, Caspase-1, and GSDMD genes. Enzyme-linked immunosorbent assay (ELISA) was performed to observe the expression of the inflammatory cytokines interleukin-1 beta (IL-1β) and IL-18. The results showed that the HBO group had a faster wound healing rate and better pathology improvement compared to the model group. The expression level of VEGF-A was higher in the HBO group compared to the model group, while the expression levels of NLRP3, Caspase-1, GSDMD, IL-1β, and IL-18 were lower than those in the model group. HBO can effectively promote the healing of chronic wounds, and the regulation of pyroptosis may be one of its mechanisms of action.

Keywords: Hyperbaric oxygen • Pyroptosis • Chronic wounds • Inflammatory

Corresponding author

Junjie Huang, School of Basic Medical Science, Youjiang Medical University for Nationalities, Baise 533000, Guangxi Zhuang Autonomous Region, China, Email: 1559199466@qq.com; Hua Wei, School of Basic Medical Science, Youjiang Medical University for Nationalities, Baise 533000, Guangxi Zhuang Autonomous Region, China, Email: 1427507023@qq.com

Introduction

Chronic wounds pose a pressing challenge in clinical practice. Traditional treatment methods such as debridement, improving circulation, and antimicrobial agents have shown limited efficacy. In recent years, with a deeper understanding of specific molecular pathways involved in wound healing, a variety of new treatment

© 2024 by the authors. Published by the Institute of Physiology of the Czech Academy of Sciences, Prague, Czech Republic

methods have been developed and applied clinically, including novel dressings, tissue-engineered skin, stem cell therapy, gene therapy, and nanotherapy [1]. The development of these treatment technologies has greatly expanded the treatment strategies for chronic wounds, leading to some breakthroughs. However, due to the high cost of treatment, these emerging therapeutic techniques have not been widely adopted in clinical practice.

Hyperbaric oxygen (HBO) therapy, a special form of physical therapy, has been widely used in the treatment of ischemic and hypoxic diseases by rapidly increasing tissue oxygen tension, improving cellular energy metabolism, and promoting cell proliferation and differentiation [2]. In recent years, with the continuous development of HBO medicine and its widespread clinical practice, its role in the treatment of chronic wounds has been widely recognized. HBO therapy can significantly shorten the healing time of wounds [3].

Pyroptosis is a newly discovered programmed cell death pathway characterized by cell swelling, plasma membrane rupture, and release of pro-inflammatory intracellular contents, playing a crucial role in the immune response to infection and inflammation [4]. Pyroptosis is mainly mediated by inflammasomes, which are multiprotein complexes that perceive pathogen-associated molecular patterns (PAMPs) and danger-associated molecular patterns (DAMPs) within cells. Upon stimulation by PAMPs or DAMPs, they rapidly assemble and subsequently activate Caspase-1 and GSDMD. GSDMD is the execution protein of pyroptosis, acting on the cell membrane to cause membrane rupture, release of cellular contents, and inflammation [5]. Currently, it is believed that there are two main signaling pathways involved in the occurrence of pyroptosis, namely, the inflammasome-dependent pathway and the inflammasome-independent pathway. NLRPs are important components of the inflammasome, among which research on NLRP1 and NLRP3 is more thorough. NLRP3 can sense various stimuli, including toxins, pathogens, crystalline substances, nucleic acids, and ATP [6], and has a wide range of biological functions, which are related to the occurrence and development of various diseases. Caspase-1 is an important regulator of pyroptosis, which is activated after assembly with NLRP3, and then cleaved into two fragments, forming a dimer, becoming mature Cleaved-Caspase-1 [7]. On the one hand, Caspase-1 cleaves the pyroptosis execution protein GSDMD at Asp275 site, forming 22 kDa GSDMD-C and 31 kDa GSDMD-N. GSDMD-N penetrates the cell membrane, forming non-selective pores with an inner diameter of about 10 to 14 nm, leading to cell swelling and apoptosis [8]. On the other hand, Caspase-1 can cleave and activate IL-1β and IL-18, which, after the formation of membrane pores, are released extracellularly through the pores, leading to pyroptosis [9]. The inflammasome-independent pathway is mediated by Caspase-4/5/11. After being stimulated by lipopolysaccharide (LPS) from intracellular gram-negative bacteria, Caspase-4/5/11 is activated and hydrolyzes its own protease. The activated Caspase-4/5/11 acts on GSDMD, forming cell membrane pores, leading to pyroptosis [5].

VX-765, also known as an interleukin-1β converting enzyme (ICE) inhibitor, is a selective inhibitor of Caspase-1. It works by binding to the active site of Caspase-1, thereby preventing the cleavage of GSDMD and pro-IL-1β [10]. VX-765 specifically targets and mitigates inflammatory responses without broadly suppressing the immune system. It has shown significant potential in reducing pyroptosis and inflammation in various disease models, indicating a promising clinical application [10] . Currently, VX-765 is widely used as a pyroptosis inhibitor in fundamental research.

Excessive or dysregulated pyroptosis is associated with the development of various diseases, including infectious diseases, autoimmune diseases, and tumors. Studies have found that in tissues of diabetic foot ulcers (DFUs), mixed bacterial infections inhibit cell proliferation, promote inflammatory responses, apoptosis, and pyroptosis. Further research showed that rod-shaped bacterial infections promote pyroptosis of polymorphonuclear leukocytes, thereby exacerbating the progression of DFUs [11]. Xiong *et al.* [12] reported that overexpression of miR-126-3p in endothelial progenitor cell (EPC)-derived exosomes can accelerate the healing of chronic wounds in diabetic rats. When transferred to human umbilical vein endothelial cells (HUVECs) injured by high glucose, cell proliferation and invasion accelerate, necrosis and apoptosis decrease, and vascular formation improves. Meanwhile, the expression of pyroptosis-related proteins Caspase-1, NRLP3, IL-1β, and IL-18 is inhibited, indicating that miR-126-3p promotes the healing of diabetic chronic wounds by suppressing endothelial pyroptosis. Another study pointed out that in HUVECs induced by tumor necrosis factor-α (TNF-α) and high glucose stimulation, overexpression of the pyroptosis key regulatory factor Caspase-1 and low expression of CD31 were observed. After treatment with N-succinylated chitosan, which has anti-inflammatory and wound healing

properties, the expression of these factors was reversed [13], further confirming the close relationship between endothelial pyroptosis and the formation of chronic wounds.

There is very limited research on the effects of HBO on pyroptosis. Recently, Ye *et al.* [14] reported that HBO alleviated oxygen-glucose deprivation-induced pyroptosis in neural stem cells (NSCs) and improved NSC proliferation and neuronal differentiation. However, how HBO affects pyroptosis of inflammatory cells (neutrophils, macrophages) and repair cells (fibroblasts, endothelial cells, keratinocytes) in wound tissue is still unknown.

Given the close relationship between pyroptosis and the formation and development of chronic wounds, as well as the unique role and efficacy of HBO in chronic wounds, this study aims to observe the effects of HBO on chronic wounds in rats and its regulatory effects on pyroptosis, exploring the mechanism by which HBO promotes the repair of chronic wounds from the perspective of pyroptosis.

Materials and Methods

Experimental animals

Forty SPF-grade male SD rats, 3 months old, weighing 220g to 250g, were provided by Changsha Tianqin Biotechnology Co., Ltd. [License Number: SCXK (Xiang) 2022-0011]. This study was approved by the Animal Ethics Committee of Youjiang Medical University for Nationalities (Animal Experimental Ethics Review Number: 2023061901).

Main reagents

VX-765 was purchased from Selleck Chemicals, USA. Antibodies against NLRP3, Caspase-1, VEGF-A, and GSDMD-N were obtained from Cell Signaling Technology, USA, while goat anti-rabbit Ig and GAPDH antibody were purchased from Beijing Zhongshan Golden Bridge Biotechnology Co., Ltd. Total RNA extraction kit was obtained from Life Technologies, and reverse transcription premix and fast antibody staining dye-based quantitative PCR premix were purchased from Molebio Biotechnology Co., Ltd. Primers for NLRP3, Caspase-1, GSDMD, and GAPDH were synthesized by Wuhan Jinkairui Biotechnology Co., Ltd. ELISA kits were purchased from Quanzhou RuiXin Biotechnology Co., Ltd. The instruments used in the experiment include: multifunctional microplate reader (SpectraMax i3x); real-time fluorescence quantitative PCR instrument (Roche LightCycler 96); fluorescence inverted microscope (Olympus IX51); transmission electron microscope (Thermo Scientific Talos F200i S/TEM).

Establishment of wound model and wound treatment method

After one week of adaptive feeding, rats were randomly divided into control group, model group, HBO group, and VX-765 group, with 10 rats in each group. After intraperitoneal injection of pentobarbital sodium at a dose of 30 mg/kg for anesthesia, rats in each group underwent a circular full-thickness skin excision with a diameter of 3 cm on the back. Subsequently, the model group, HBO group, and VX-765 group received intramuscular injection of 80mg/kg hydrocortisone acetate in the thigh muscles to establish a chronic wound model [15, 16], while the control group did not receive hydrocortisone acetate injection, forming an acute wound. After the wound model was established, each group received dressing changes twice daily. In addition to dressing changes, no other treatment measures were taken for the control group and model group. The HBO group received HBO therapy using a HBO chamber (GY-3200, Yantai Hongyuan) after the second dressing change each day. The HBO treatment protocol was as follows: 15 minutes of pressurization, 60 minutes of stable pressure, 15 minutes of depressurization, with pure oxygen inhalation throughout the entire treatment process. The total treatment time was 90 minutes, and the treatment pressure was 2 atmospheres absolute (ATA), once per day. The VX-765 group received a daily intraperitoneal injection of VX-765 at a dose of 50 mg/kg [17]. Rats from each group were anesthetized with an intraperitoneal injection of 30mg/kg pentobarbital sodium 4 hours after completing the 7th day of treatment. After collecting wound tissue specimens, rats were euthanized using cervical dislocation.

Recording wound area

After successful model creation, each rat was marked using ear tagging. Four hours after completing the 7th day of treatment, digital photographs of the wounds were taken with a digital camera positioned perpendicular to the wounds, and Image J software was used to measure the wound area and calculate the healing rate. The wound healing rate was calculated as follows: (original wound area - unhealed wound area) / original wound area × 100 %.

HE staining to observe the pathological structure of wound tissues

The collected wound tissues were immediately fixed in 10 % formaldehyde, dehydrated in ethanol of gradient concentrations, and then cleared with xylene. The cleared tissue blocks were sequentially immersed in paraffin with different melting points to replace the xylene. Subsequently, embedding, sectioning, baking, and HE staining were performed. After slide preparation, the specimens were observed under a light microscope to assess re-epithelialization, granulation tissue formation, and angiogenesis, and quantitative analysis was conducted based on the histological changes of wound tissues [18], as shown in Tables 1-3. The total score for each specimen was the sum of the scores from the following three parts, with higher scores indicating more obvious tissue improvement.

Transmission electron microscopy to observe cellular ultrastructure

Samples were fixed overnight in 2.5 % glutaraldehyde solution at 4 °C, and the next day, glutaraldehyde solution was discarded, and the samples were washed three times. The samples were then fixed in 1 % osmium tetroxide solution for 1-2 hours. After discarding osmium tetroxide solution, the samples were washed and dehydrated in a gradient concentration of ethanol solution. After dehydration, the samples were rapidly transferred to a mixture of acetone and embedding agent in equal volume, immersed for 30 minutes, and then transferred to pure embedding agent for overnight immersion, followed by embedding. The samples were sliced into 70-90nm sections using an ultrathin slicer, stained with uranyl acetate and lead citrate for 15 minutes each, and observed for changes in cellular ultrastructure under a transmission electron microscope.

Immunofluorescence staining to observe the expression and localization of pro-angiogenic and pro-pyroptotic proteins

Tissue sections were successively treated with xylene, ethanol, and deionized water, and then subjected to high-pressure repair with 0.01M sodium citrate buffer using a pressure cooker. The tissue sections were then blocked with 5 % BSA blocking solution at room temperature for 30 minutes. After removing the blocking solution, the primary antibodies, including rabbit anti-VEGF-A and rabbit anti-GSDMD-N, were added and incubated overnight at 4 °C. The next day, the tissue sections were washed and incubated with secondary antibodies at room temperature for 1 hour. After washing and drying, DAPI staining solution was added and incubated at room temperature for 5 minutes. After washing again and drying, the slides were sealed with mounting solution. The staining of cells was observed under a fluorescence microscope, and Image J software was used to determine the average fluorescence intensity for comparative analysis.

Table 1. Scoring of re-epithelialization in wound healing

Score	Re-epithelialization
0	Absent
1	Little epithelial proliferation, crusting
2	Moderate re-epithelialization, spongiosis, subepithelial edema
3	Complete remodeling

Table 2. Scoring of granulation formation in wound healing

Score	Granulation tissue
0	Inflammatory tissue
1	Immature and inflammatory tissue, edema
2	Minimal to moderate organization and collagen deposition, slight inflammation
3	Dense tissue and collagen matrix deposition
4	Complete remodeling

Table 3. Scoring of angiogenesis in wound healing

Score	Angiogenesis
0	Absence of angiogenesis, inflammation, and hemorrhage
1	1–2 capillaries per site, fibrin deposition, edema, hemorrhage, congestion
2	3–4 capillaries per site, moderate edema and congestion
3	5–6 capillaries per site, slight edema and congestion
4	More than 7 capillaries per site

Table 4. The primer sequences of RT-qPCR

Gene	Primer sequences
NLRP3	Forward: 5′-TGAACAGACGCTACACCC-3′
	Reverse: 5′-CATCCTCAGGCTCAAAGA-3′
Caspase-1	Forward: 5′-AAGACAAGCCCAAGGTTA-3′
	Reverse: 5′-GTTGAAGAGCAGAAAGCA-3′
GSDMD	Forward: 5′-ATTGGCTCTGAATGGGATA-3′
	Reverse: 5′-GTACGGCAAGCAGACTAAA-3′
GAPDH	Forward: 5′-CAGGAGGCATTGCTGATGAT-3′
	Reverse: 5′-GAAGGCTGGGGCTCATTT-3′

Detection of pro-angiogenic and pro-pyroptotic expression by western blot

Total protein was extracted using tissue lysis buffer, and protein quantification was performed according to the BCA method. Samples were boiled for 10 minutes to denature the proteins and stored at -80 °C for subsequent experiments. SDS-PAGE gels were prepared, and protein samples were loaded at 10 μg per well. The concentrated gel was electrophoresed at a constant voltage of 60V, and the separating gel was electrophoresed at a constant voltage of 120V. After electrophoresis, proteins were transferred onto a membrane using a wet transfer method. The membrane was then blocked with 50 g/L skim milk blocking solution at room temperature for 1 hour, followed by incubation with primary antibodies, including rabbit anti-VEGF-A, rabbit anti-NLRP3, rabbit anti-Caspase-1, and rabbit anti-GSDMD-N, overnight at 4 °C. The next day, the membrane was incubated with secondary antibodies at room temperature for 1 hour, followed by visualization and analysis of grayscale values using Image J software to calculate the relative expression levels.

Detection of pro-pyroptotic gene expression by qRT-PCR

Total RNA from wound tissues of each group was extracted using the Trizol method, and the concentration and purity of total RNA were determined. Only samples with OD260/OD280 ratios within the range of 1.8 to 2.0 were used for subsequent detection. Reverse transcription was performed according to the reverse transcription kit method, followed by PCR amplification of the resulting cDNA. The reaction program was as follows: pre-denaturation at 95 °C for 15 minutes, followed by 40 cycles of PCR reaction, each cycle including denaturation at 95 °C for 10 seconds and annealing/extension at 60 °C for 20 seconds. GAPDH was used as the reference gene, and the target genes were NLRP3, Caspase-1, and GSDMD, with primer sequences shown in Table 4. The Ct values were converted using the formula $F = 2^{-\Delta\Delta Ct.}$

ELISA to detect levels of inflammatory cytokines

Cut 50 mg of tissue from each specimen and homogenize using a homogenizer, centrifuged to collect the supernatant for testing. Allow the reagents to equilibrate at room temperature for 30 minutes before the experiment. Standard samples and test samples were added to pre-set standard wells and test sample wells,

respectively, each well with 50 µl, followed by adding 100 µl of horse radish peroxidase (HRP) labeled antibody to each well, incubated in a 37 °C incubator for 1 hour, followed by discarding the liquid in the wells and washing. Substrate solution (100 µl) was added, incubated at 37 °C in the dark for 15 minutes. Finally, 50 µl of stop solution was added to terminate the reaction. The OD values at 450 nm were measured using an enzyme immunoassay analyzer.

Statistical analysis

Data were analyzed using SPSS 25.0 software. Normally distributed data were expressed as mean ± standard deviation (SD), and one-way analysis of variance (ANOVA) was used for intergroup comparison; non-normally distributed data were expressed as Median (Interquartile Range), and the Mann-Whitney U test was used for analysis, with $p<0.05$ suggesting statistically significant differences.

Results

HBO accelerates healing of chronic wounds

In the control group, HBO group, and VX-765 group, the wounds showed slight redness and swelling, with a few areas covered by necrotic tissue. After clearing the necrotic tissue, visibly red granulation tissue formed. In the model group, the wounds was ulcerated with a large amount of exudate and has not formed obvious granulation tissue. Most of the wounds in the control group, HBO group, and VX-765 group re-epithelialized, while re-epithelialization was delayed in the model group (Fig. 1A). The analysis of wound healing rates shows that after HBO treatment, the wound healing speed in rats was significantly accelerated. The wound healing rate in the HBO group was 46.94% higher than that in the model group (43.67±9.47% and 64.17±9.96%, Model and HBO, respectively; $p=0.0001$). The wound healing speed in the control group and VX-765 group was also faster than that in the model group ($p<0.0001$ and $p=0.0028$, respectively) (Fig. 1B).

HBO improves the pathological status of chronic wound tissues

Histopathological examination by HE staining, as shown in Fig. 2A, revealed varying degrees of edema and inflammation cell infiltration dominated by neutrophils in each group, most pronounced in the model group. The control group, HBO group, and VX-765 group showed abundant granulation tissue formation, with scattered newly formed capillaries within the granulation tissue. In the control group, fibroblasts were densely arranged, while in the HBO group and VX-765 group, fibroblast arrangement was sparse and disordered, and no obvious granulation tissue was formed in the model group. Quantitative analysis showed that the histological scores in the HBO group were higher than those in the model group (2.33±0.58 and 5.00±1.00, Model and HBO, respectively; $p=0.01$) (Fig. 2B). Transmission electron microscopy revealed scattered pyroptosic cells in the model group, with severe cellular structural damage, nuclear shrinkage in some cells, dissolution of the cell membrane, and leakage of cellular contents. The number of pyroptosic cells in the wound tissues of the control group, HBO group, and VX-765 group was significantly lower than that in the model group. The ultrastructure of the pyroptosic cells mainly showed varying degrees of cell and mitochondrial swelling, discontinuity of the cell membrane, or bubble-like protrusions (necrotic bodies) on the cell membrane (Fig. 2C). These findings suggest that HBO improves the pathological status of chronic wound tissues.

HBO promotes the expression of pro-angiogenic factor

To further explore the effects of HBO on chronic wound healing at the molecular level, we used immunofluorescence and Western blot assays to determine the expression of the main pro-angiogenic molecule VEGF-A in wound tissues of each group. The results show that VEGF-A was positively expressed in the cytoplasm of wound tissue cells in all groups. The average fluorescence intensity of VEGF-A in the HBO group was 51.65 % higher than that in the model group (19.05±3.56 and 28.89±2.47, Model and HBO, respectively; $p=0.012$) (Fig. 3A), and the expression of VEGF-A protein was 39.39 % higher than that in the model group (0.66±0.06 and 0.92±0.06, Model and HBO, respectively; $p=0.013$) (Fig. 3B). This suggests that HBO promotes the expression of VEGF-A. Additionally, compared with the control group, the model group showed low expression of VEGF-A, and its expression increased after VX-765 intervention (all $p<0.05$) (Fig. 3A-B).

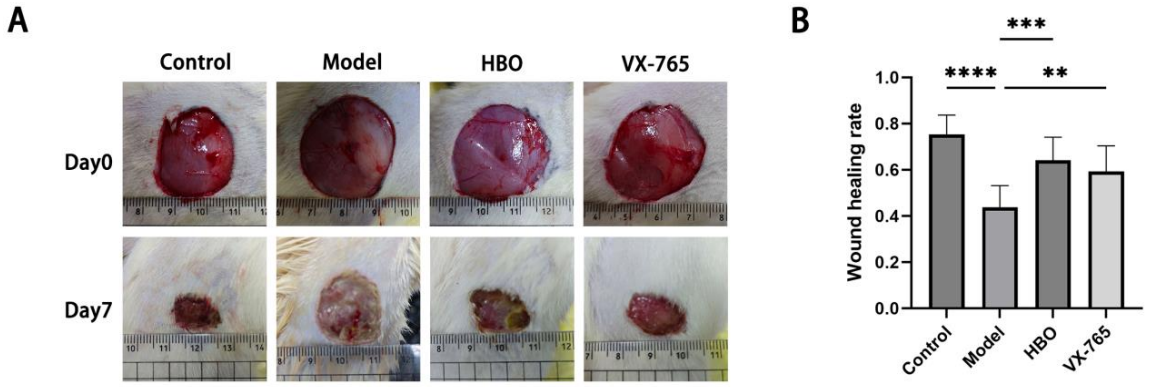

Fig. 1. Acceleration of chronic wound healing by HBO. (**A**) Comparison of wound healing status in the four groups: the control group, HBO group, and VX-765 group showed reddish wounds with mostly re-epithelialization, while the model group had significant adherence of necrotic tissue and delayed re-epithelialization. (**B**) Comparison of wound healing rates among the four groups. Results are expressed as the mean±SD with n=10 per group. *p<0.05，**p<0.01，***p<0.001，****p<0.0001 vs model group.

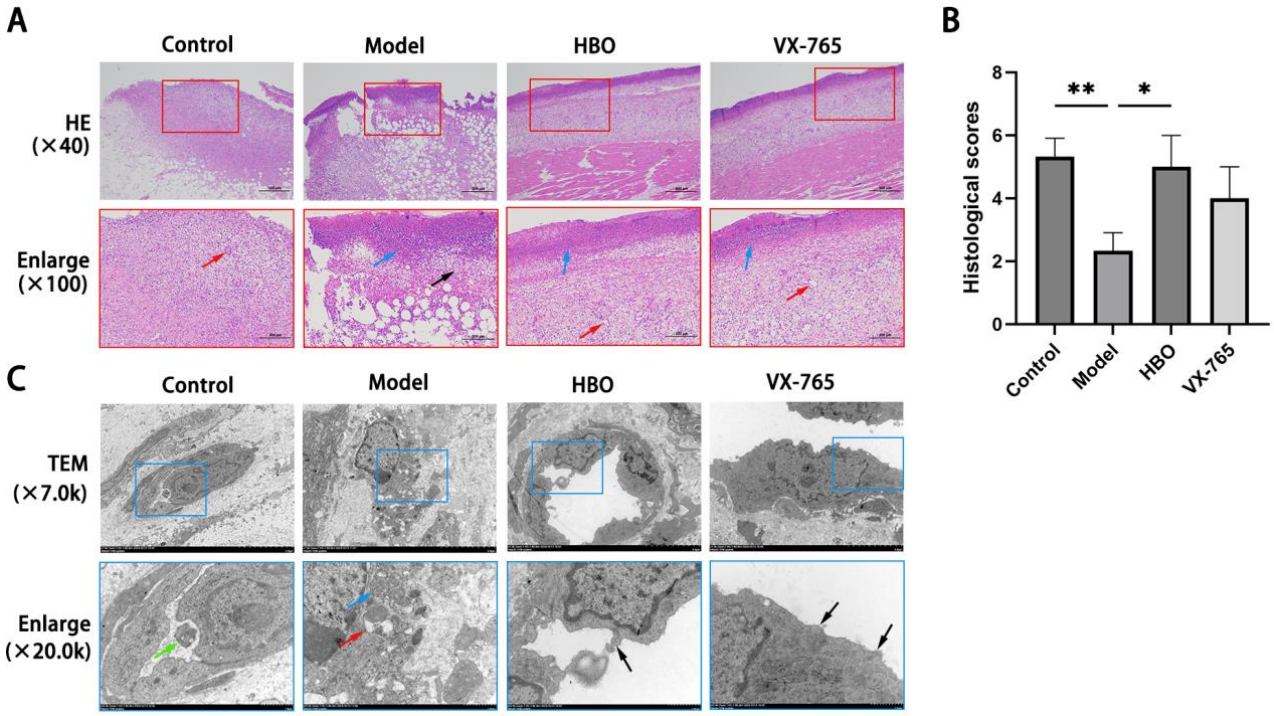

Fig. 2. Improvement of the pathological status of chronic wound tissues by HBO. (**A**) Histopathological status of wounds stained with HE in the four groups: the control group showed the formation of a significant capillary network (red arrow); the model group exhibited marked edema (black arrow) and extensive infiltration of inflammatory cells (blue arrow), with no observed neovascularization; in the HBO group and VX-765 group, inflammatory cell infiltration (blue arrow) and scattered distribution of newly formed capillaries (red arrow) were visible. (**B**) Comparison of histological scores of wound tissues in the four groups. (**C**) Ultrastructural images of wound tissues in the four groups: In the control group, HBO group, and VX-765 group, cell structures are minimally disrupted, with clear cell membranes. Pores are observed on the cell membrane in the control group (green arrow), while protrusions on the cell membrane, indicating pyroptotic bodies, are visible in the HBO group and VX-765 group (black arrow). In the model group, cell structures are severely disrupted, showing cytoplasmic vacuolization, mitochondrial swelling (blue arrow), autophagosome formation (red arrow), cell membrane dissolution, and release of intracellular contents. Results are expressed as the mean±SD with n=3 per group. *p<0.05，**p<0.01，***p<0.001，****p<0.0001 vs model group.

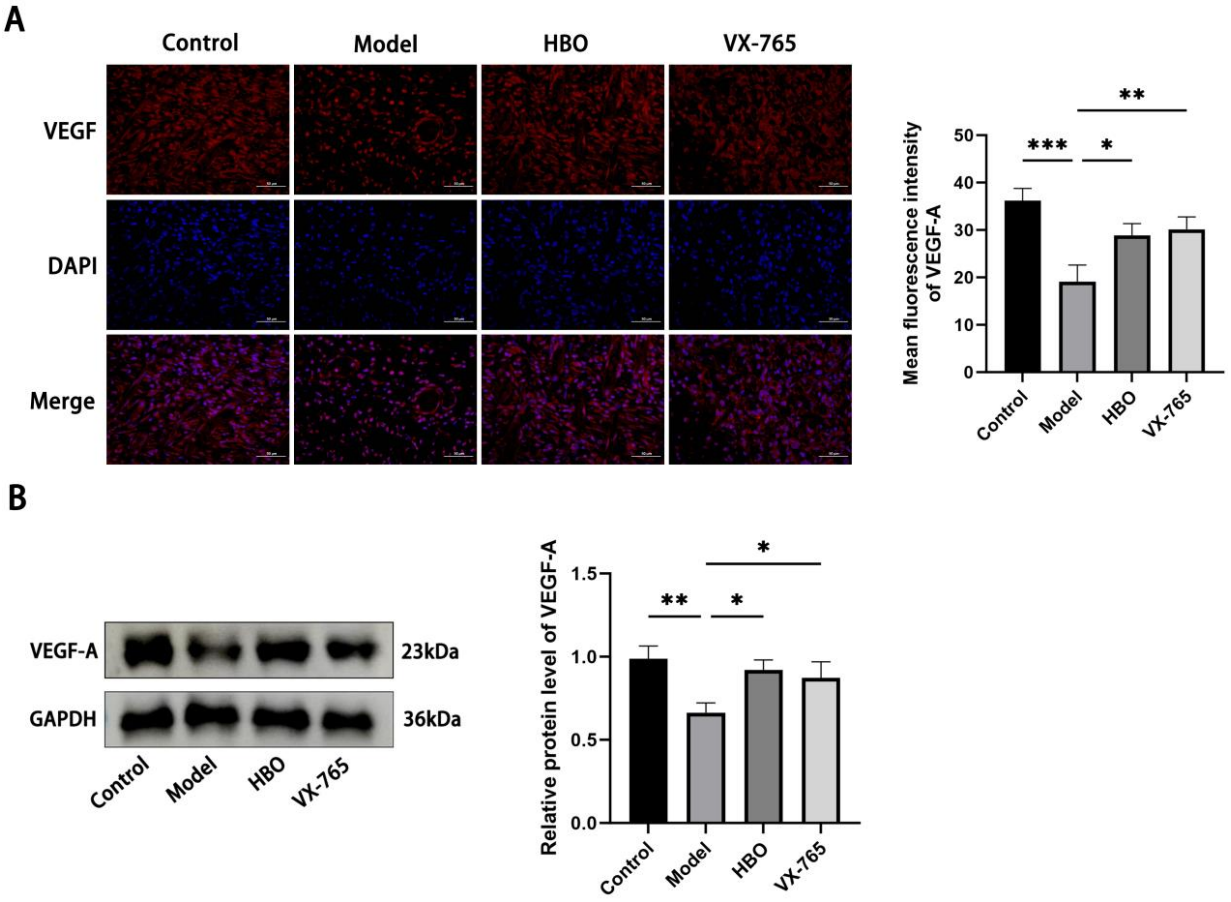

Fig. 3. HBO promotes the expression of pro-angiogenic factor. (**A**) Immunofluorescence assay to measure the expression of VEGF-A. (**B**) Western blot assay to measure the expression of VEGF-A. Results are expressed as the mean±SD with n=3 per group。*p<0.05，**p<0.01，***p<0.001，****p<0.0001vs model group.

HBO suppresses the expression of pro-pyroptotic factors.

To investigate the changes in pyroptosis in chronic wound tissues and the effects of HBO on the expression of pyroptosis-related molecules, we used immunofluorescence to detect the expression and localization of GSDMD-N in wound tissue cells, Western blot to detect the expression of pro-pyroptotic proteins NLRP3, Caspase-1, and GSDMD-N, and qRT-PCR to detect the expression of pro-pyroptotic genes NLRP3, Caspase-1, and GSDMD. Immunofluorescence showed that GSDMD-N was positively expressed to varying degrees in the cytoplasm of tissue cells. Further quantitative analysis using Image J software showed that the average fluorescence intensity of GSDMD-N in the HBO group was significantly lower than that in the model group (37.16±2.52 and 24.59±1.34, Model and HBO, respectively; p=0.0002) (Fig. 4A). Western blot analysis revealed that, compared to the model group, the expression of NLRP3 in the HBO group decreased by 23.4 % (0.94±0.05 and 0.72±0.05, Model and HBO, respectively; p=0.011), Caspase-1 decreased by 40.71 % (1.13±0.13 and 0.67±0.06, Model and HBO, respectively; p=0.001), and GSDMD-N decreased by 20.95 % (1.05±0.03 and 0.83±0.08, Model and HBO, respectively; p=0.024) (Fig. 4B). Similarly, after HBO treatment, the expression of NLRP3, Caspase-1, and GSDMD mRNA was also downregulated. Compared to the model group, NLRP3 mRNA expression decreased by 58.73 % (3.78±0.11 and 1.56±0.06, Model and HBO, respectively; p<0.0001), Caspase-1 mRNA decreased by 67.37 % (2.85±0.53 and 0.93±0.03, Model and HBO, respectively; p=0.0003), and GSDMD mRNA decreased by 60.65 % (2.16±0.20 and 0.85±0.06, Model and HBO, respectively; p<0.0001) (Fig. 4C). VX-765 exerted effects similar to HBO, inhibiting the expression of NLRP3, Caspase-1, and GSDMD at both the protein and gene levels (all p<0.05) (Fig. 4A-C).

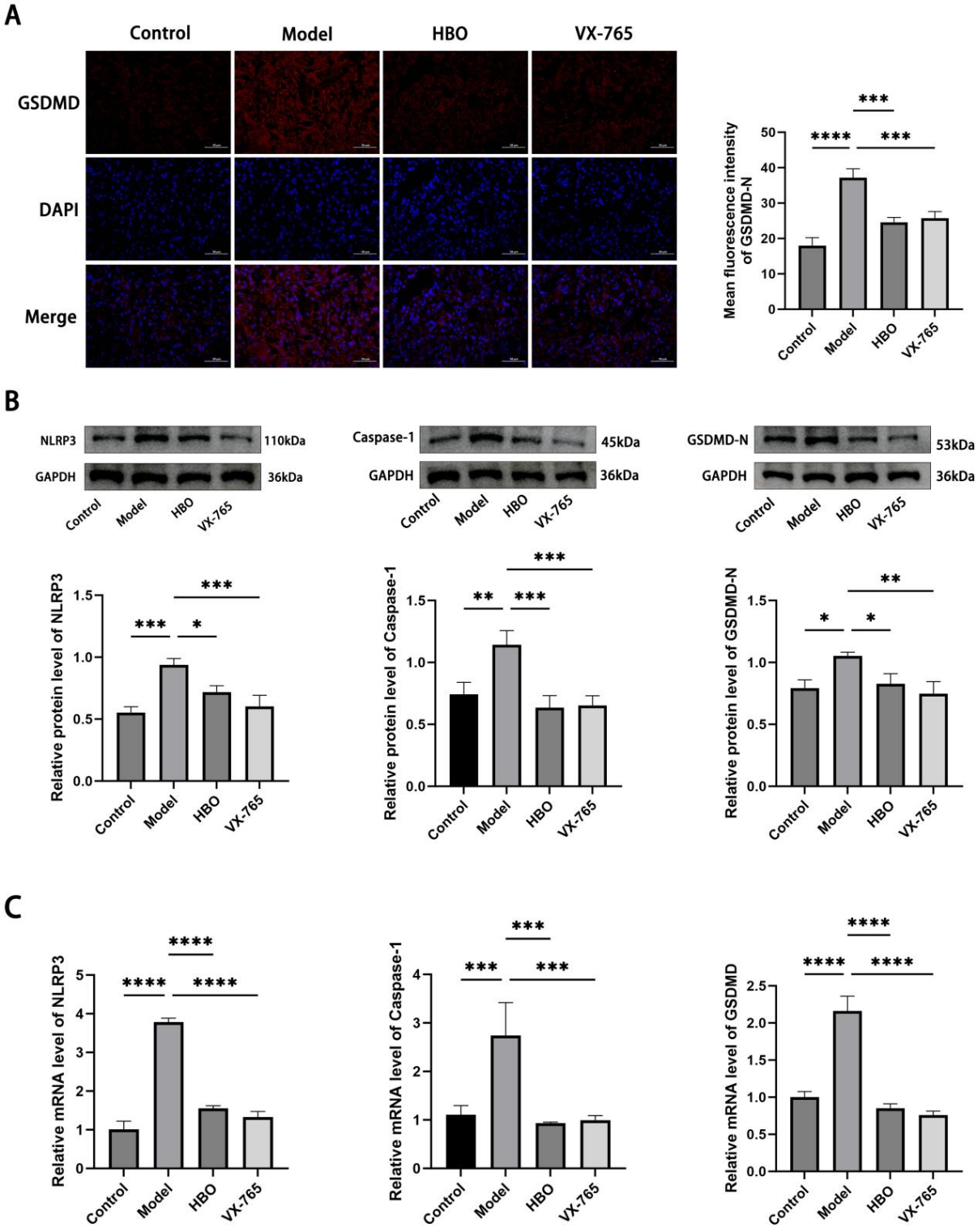

Fig. 4. HBO suppresses the expression of pro-pyroptotic factors. (**A**) Immunofluorescence assay to detect the expression of GSDMD-N. (**B**) Western blot assay to detect the expression of NLRP3, Caspase-1, and GSDMD-N proteins. (**C**) qRT-PCR assay to detect the expression of NLRP3, Caspase-1, and GSDMD mRNA. Results are expressed as the mean±SD with n=3 per group。*p<0.05，**p<0.01，***p<0.001，****p<0.0001 vs model group.

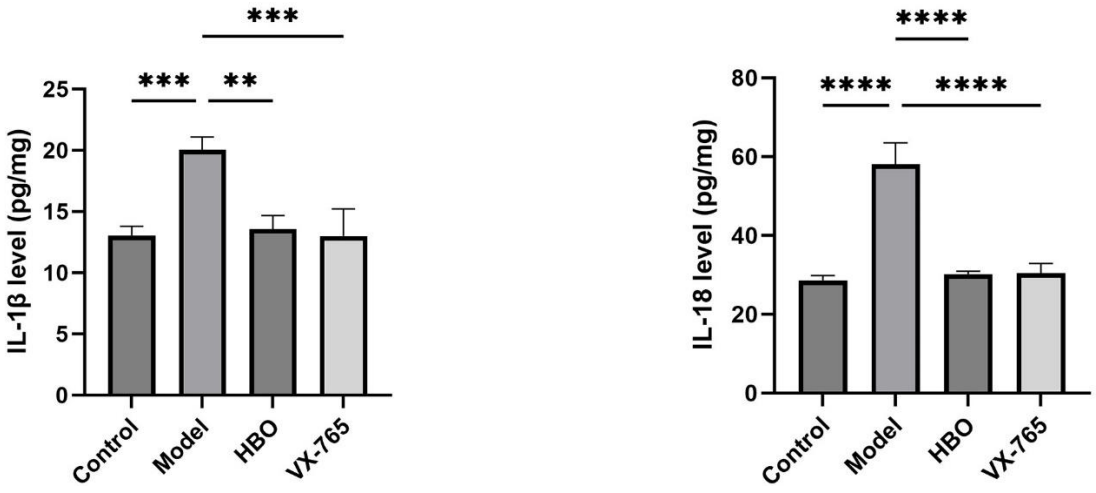

Fig. 5. HBO inhibits the synthesis of inflammatory factors. ELISA was used to determine the expression of IL-1β and IL-18. Results are expressed as the mean ± SD with n=3 per group. *p<0.05，**p<0.01，***p<0.001，****p<0.0001 vs model group.

HBO inhibits the synthesis of inflammatory factors

IL-1β and IL-18 are direct products of pyroptosis, reflecting the inflammatory status of the tissue. In this study, we extracted wound tissues from each group for ELISA testing to determine the expression of IL-1β and IL-18. The results showed that the expression of IL-1β in the HBO group was 32.26 % lower compared to the model group (20.05±1.04 and 13.58±1.10, Model and HBO, respectively; p=0.0012). Similarly, the expression of IL-18 was 47.94 % lower in the HBO group compared to the model group (58.06±5.53 and 30.23±0.74, Model and HBO, respectively; p<0.0001). This indicates that HBO inhibited the expression of IL-1β and IL-18. Additionally, we observed that the expression levels of IL-1β and IL-18 in the control group and VX-765 group were also lower than those in the model group (all p<0.001) (Fig. 5).

Discussion

The outcome of pyroptosis includes cell death and inflammation activation. HBO has long been proven to counteract apoptosis in wound tissues and improve wound inflammation [19]. However, whether pyroptosis, also a form of programmed cell death, is regulated by HBO in wound tissues remains unknown. It is also unclear whether HBO's regulatory effect on wound inflammation is mediated by pyroptosis. We are conducting this study precisely to answer these questions, aiming to reveal the effects and mechanisms of HBO on pyroptosis in chronic wound tissues.

Observations of wound healing, wound healing rate analysis, and pathological examination show that the improvement of wounds in the HBO group is superior to the model group. VEGF-A is a highly specific molecule that promotes the migration, proliferation, and angiogenesis of vascular endothelial cells. The expression level of VEGF-A in the HBO group is also significantly higher than that in the model group, indicating that HBO promotes the repair of chronic wounds, which is consistent with previous research conclusions. It is believed that HBO can rapidly improve the blood oxygen partial pressure of wounds, and the increase in adenosine triphosphate (ATP) synthesized by oxidative phosphorylation drives cell mitosis, promotes the proliferation of wound fibroblasts and the angiogenic ability of vascular endothelial cells. Additionally, HBO induces the expression of key molecules promoting wound healing, including hypoxia-inducible factor -1 alpha (HIF-1α), nuclear factor kappa-B (NF-κB), VEGF-A, stromal cell-derived factor 1 (SDF-1), and chemokine (C-X-C motif) receptor 4 (CXCR4) [20]. Reactive oxygen species (ROS) are byproducts of oxygen metabolism mainly produced by oxidative phosphorylation, and mitochondrial nicotinamide adenine dinucleotide phosphate hydrogen (NADPH) oxidase and xanthine oxidase (XOD) can also catalyze ROS generation. Although short-term hypoxia can stimulate ROS synthesis in acute wounds, the synthesis of ROS is inhibited in chronic wounds [21]. HBO therapy can increase systemic ROS levels. ROS, as the second messenger to maintain cellular life activities, plays a crucial role in promoting cell proliferation, migration, and angiogenesis in wound repair [3]. Additionally, it has been confirmed that ROS is beneficial for mobilizing stem cells to wound sites [22]. However,

high levels of ROS can damage cell structures such as lipids, proteins, and DNA, affecting cell membrane permeability and osmoregulation, leading to apoptosis or accelerated cell senescence [23]. It was previously believed that HBO could lead to ROS accumulation, disrupt cell homeostasis, and was considered a potential side effect of HBO. Recent studies have shown that routine HBO treatment not only does not cause ROS accumulation and oxidative stress but also strongly mobilizes the antioxidant enzyme system, greatly improving the defense against oxidative damage [24, 25].

Transmission electron microscopy showed that the number of pyroptotic cells in the model group was higher than that in the control group. Meanwhile, the expression of pro-pyroptotic factors NLRP3, Caspase-1, GSDMD, and inflammatory factors IL-1β and IL-18 in the model group was also higher than that in the control group, suggesting that compared with acute wounds, the pyroptosis of cells in chronic wound tissues intensifies, leading to a more pronounced inflammatory response. Chronic wounds include diabetic foot ulcers, pressure ulcers, lower limb venous ulcers, radiation injuries, etc., which are common in patients with diabetes, cancer, long-term bed rest, and steroid use. The formation mechanism is complex, with tissue chronic ischemia, hypoxia, and prolonged infection as the main pathophysiological changes [26]. Therefore, we believe that hypoxia and chronic infection are the main reasons for increased pyroptosis of wound cells. Hypoxia and the resulting ATP deficiency act as intrinsic DAMPs, which are recognized by cytosolic pattern recognition receptors (PRRs) and activate downstream signaling pathways, thereby initiating inflammasome assembly. NLRP3 inflammasome is an important component of innate immunity, which can be activated by various pathogens or danger signals. Activated NLRP3 cleaves Caspase-1, initiating the inflammasome-dependent pyroptotic pathway [5]. Oxygen plays an important role in the body's anti-infective immunity. In chronic wound tissues, hypoxia leads to impaired function of inflammatory cells such as neutrophils and macrophages, often resulting in persistent infection [26]. PAMPs on the pathogen's surface act as ligands for PRRs. After mutual recognition, they activate the classical cell pyroptosis pathway through inflammasome mediation in the same manner [5]. In wounds infected with Gram-negative bacteria, LPS can be directly recognized by Caspase-11/4/5, activating the pyroptotic process through the inflammasome-independent pathway [5, 27]. Pyroptosis is an immune activation mechanism. During the inflammatory phase of wound healing, the inflammatory response mediated by pyroptosis plays a positive role in eliminating infections. However, pyroptosis, as a double-edged sword, excessive pyroptosis can lead to excessive and harmful inflammatory responses [28]. Therefore, the long-term uncontrolled inflammation in chronic wounds may be related to excessive pyroptosis to a certain extent.

After HBO treatment, the number of pyroptotic cells in wound tissues decreased, and the expression of NLRP3, Caspase-1, GSDMD, IL-1β, and IL-18 was downregulated, indicating that HBO inhibited pyroptosis in wound cells. Under HBO conditions, the blood oxygen pressure and oxygen diffusion distance in wound tissues significantly increased, leading to an increase in ATP synthesis in wound cells due to the improvement of hypoxia. This stimulation weakened the danger signals of PRRs, thus inhibiting pyroptosis. In addition, HBO has been proven to have a significant antibacterial effect, effectively controlling wound infection and reducing pyroptosis induced by PAMPs after HBO treatment. HBO may exert its antibacterial effect through multiple mechanisms. Firstly, the increase in tissue oxygen pressure itself is believed to directly inhibit the growth and reproduction of anaerobic microorganisms, especially strains of Clostridium perfringens [29]. Secondly, after exposure to HBO, the phagocytosis of pathogens by macrophages, neutrophils, and dendritic cells is enhanced. At the same time, cellular respiration bursts produce large amounts of ROS. ROS, as toxic molecules, create a toxic oxidative stress environment inside phagocytes, causing damage to the DNA, lipid peroxidation, and oxidation of amino acids of engulfed pathogens [30]. Thirdly, HBO induces aerobic metabolism to activate dormant bacteria, thereby increasing the sensitivity of some antibiotics [31].

In summary, HBO can effectively promote the healing of chronic wounds, and the inhibition of cell pyroptosis in wound tissues may be one of its mechanisms of action.

Limitations

The ZDF rat is one of the most ideal experimental animals for establishing a chronic wound model. Due to limited conditions, we were unable to use the ZDF rat as a research subject, which is very regrettable. The wound healing process involves the coordinated participation of various cells with different functions. Therefore, further verification is needed through cell culture and in vitro studies to investigate the effects of HBO on the pyroptosis

of individual tissue cells.

Conflict of Interest

There is no conflict of interest.

Acknowledgements

This work was supported by Baise Regional Joint Special Program for Common Diseases (Baike 20224118) and Guangxi Medical and Health Appropriate Technology Development and Promotion Application Project (S2023111).

References

1. Kolimi P, Narala S, Nyavanandi D, Youssef A, Dudhipala N: Innovative Treatment Strategies to Accelerate Wound Healing: Trajectory and Recent Advancements. Cells-Basel 2022; 11. https://doi.org/10.3390/cells11152439
2. Madero J, Salvador M, Kadouch J, Munoz-Gonzalez C, Fakih-Gomez N: Role of Hyperbaric Oxygen in Filler-Induced Vascular Occlusion. Aesthet Plast Surg 2024. https://doi.org/10.1007/s00266-024-03920-7
3. Ruzicka J, Dejmek J, Bolek L, Benes J, Kuncova J: Hyperbaric oxygen influences chronic wound healing - a cellular level review. Physiol Res 2021; 70:S261-S273. https://doi.org/10.33549/physiolres.934822
4. Xu P, Li F, Tang H: Pyroptosis and airway homeostasis regulation. Physiol Res 2023; 72:1-13. https://doi.org/10.33549/physiolres.934971
5. Yu P, Zhang X, Liu N, Tang L, Peng C, Chen X: Pyroptosis: mechanisms and diseases. Signal Transduct Tar 2021; 6:128. https://doi.org/10.1038/s41392-021-00507-5
6. Swanson KV, Deng M, Ting JP: The NLRP3 inflammasome: molecular activation and regulation to therapeutics. Nat Rev Immunol 2019; 19:477-489. https://doi.org/10.1038/s41577-019-0165-0
7. Sollberger G, Strittmatter GE, Garstkiewicz M, Sand J, Beer HD: Caspase-1: the inflammasome and beyond. Innate Immun-London 2014; 20:115-125. https://doi.org/10.1177/1753425913484374
8. Sborgi L, Ruhl S, Mulvihill E, Pipercevic J, Heilig R, Stahlberg H, Farady CJ et al: GSDMD membrane pore formation constitutes the mechanism of pyroptotic cell death. Embo J 2016; 35:1766-1778. https://doi.org/10.15252/embj.201694696
9. Liu X, Zhang Z, Ruan J, Pan Y, Magupalli VG, Wu H, Lieberman J: Inflammasome-activated gasdermin D causes pyroptosis by forming membrane pores. Nature 2016; 535:153-158. https://doi.org/10.1038/nature18629
10. Modi P, Shah BM, Patel S: Interleukin-1beta converting enzyme (ICE): A comprehensive review on discovery and development of caspase-1 inhibitors. Eur J Med Chem 2023; 261:115861. https://doi.org/10.1016/j.ejmech.2023.115861
11. Zheng H, Na H, Yao J, Su S, Han F, Li X, Chen X: 16S rRNA seq-identified Corynebacterium promotes pyroptosis to aggravate diabetic foot ulcer. Bmc Infect Dis 2024; 24:366. https://doi.org/10.1186/s12879-024-09235-x
12. Xiong W, Zhang X, Zhou J, Chen J, Liu Y, Yan Y, Tan M et al: Astragaloside IV promotes exosome secretion of endothelial progenitor cells to regulate PI3KR2/SPRED1 signaling and inhibit pyroptosis of diabetic endothelial cells. Cytotherapy 2024; 26:36-50. https://doi.org/10.1016/j.jcyt.2023.08.013
13. Chen Z, Yuan M, Li H, Li L, Luo B, Lu L, Xiang Q et al: Succinylated chitosan derivative restore HUVEC cells function damaged by TNF-alpha and high glucose in vitro and enhanced wound healing. Int J Biol Macromol 2024; 265:130825. https://doi.org/10.1016/j.ijbiomac.2024.130825
14. Ye Y, Feng Z, Tian S, Yang Y, Jia Y, Wang G, Wang J et al: HBO Alleviates Neural Stem Cell Pyroptosis via lncRNA-H19/miR-423-5p/NLRP3 Axis and Improves Neurogenesis after Oxygen Glucose Deprivation. Oxid Med Cell Longev 2022; 2022:9030771. https://doi.org/10.1155/2022/9030771
15. Xu JN, Que HF, Tang HJ: Effects and action mechanisms of Buyang Huanwu Decoction in wound healing of chronic skin ulcers of rats. Zhong Xi Yi Jie He Xue Bao 2009; 7:1145-1149. https://doi.org/10.3736/jcim20091210
16. Yadav VP, Shukla A, Choudhury S, Singh R, Anand M, Prabhu SN: IL1beta/ TNFalpha/COX-2/VEGF axis responsible for effective healing potential of C-glucoside xanthone (mangiferin) based ointment in immunocompromised rats. Cytokine 2022; 158:156012. https://doi.org/10.1016/j.cyto.2022.156012

17. Shields CA, Tardo GA, Wang X, Peacock G, Robbins M, Glenn H, Wilson R et al: Inhibition of Caspase 1 Reduces Blood Pressure, Cytotoxic NK Cells, and Inflammatory T-Helper 17 Cells in Placental Ischemic Rats. Int J Mol Sci 2024; 25. https://doi.org/10.3390/ijms25020863
18. Altavilla D, Galeano M, Bitto A, Minutoli L, Squadrito G, Seminara P, Venuti FS et al: Lipid peroxidation inhibition by raxofelast improves angiogenesis and wound healing in experimental burn wounds. Shock 2005; 24:85-91. https://doi.org/10.1097/01.shk.0000168523.37796.89
19. Lindenmann J, Kamolz L, Graier W, Smolle J, Smolle-Juettner FM: Hyperbaric oxygen therapy and tissue regeneration: a literature survey. Biomedicines 2022; 10. https://doi.org/10.3390/biomedicines10123145
20. Huang X, Liang P, Jiang B, Zhang P, Yu W, Duan M, Guo L et al: Hyperbaric oxygen potentiates diabetic wound healing by promoting fibroblast cell proliferation and endothelial cell angiogenesis. Life Sci 2020; 259:118246. https://doi.org/10.1016/j.lfs.2020.118246
21. Gottrup F, Dissemond J, Baines C, Frykberg R, Jensen PO, Kot J, Kroger K et al: Use of Oxygen Therapies in Wound Healing. J Wound Care 2017; 26:S1-S43. https://doi.org/10.12968/jowc.2017.26.Sup5.S1
22. Dunnill C, Patton T, Brennan J, Barrett J, Dryden M, Cooke J, Leaper D et al: Reactive oxygen species (ROS) and wound healing: the functional role of ROS and emerging ROS-modulating technologies for augmentation of the healing process. Int Wound J 2017; 14:89-96. https://doi.org/10.1111/iwj.12557
23. Schafer M, Werner S: Oxidative stress in normal and impaired wound repair. Pharmacol Res 2008; 58:165-171. https://doi.org/10.1016/j.phrs.2008.06.004
24. Mrakic-Sposta S, Vezzoli A, Garetto G, Paganini M, Camporesi E, Giacon TA, Dellanoce C et al: Hyperbaric oxygen therapy counters oxidative stress/inflammation-driven symptoms in long COVID-19 patients: preliminary outcomes. Metabolites 2023; 13. https://doi.org/10.3390/metabo13101032
25. Cannellotto M, Yasells GA, Landa MS: Hyperoxia: Effective Mechanism of Hyperbaric Treatment at Mild-Pressure. Int J Mol Sci 2024; 25. https://doi.org/10.3390/ijms25020777
26. Yang Z, Ren K, Chen Y, Quanji X, Cai C, Yin J: Oxygen-generating hydrogels as oxygenation therapy for accelerated chronic wound healing. Adv Healthc Mater 2024; 13:e2302391. https://doi.org/10.1002/adhm.202302391
27. Wang F, Ye J, Zhu W, Ge R, Hu C, Qian Y, Li Y et al: Galectin-3 mediates endotoxin internalization and caspase-4/11 activation in tubular epithelials and macrophages during sepsis and sepsis-associated acute kidney injury. Inflammation 2024; 47:454-468. https://doi.org/10.1007/s10753-023-01928-w
28. Liu Z, Wang C, Lin C: Pyroptosis as a double-edged sword: The pathogenic and therapeutic roles in inflammatory diseases and cancers. Life Sci 2023; 318:121498. https://doi.org/10.1016/j.lfs.2023.121498
29. Wijesooriya LI, Waidyathilake D: Antimicrobial properties of nonantibiotic agents for effective treatment of localized wound infections: a minireview. int j low extr wound 2022; 21:207-218. https://doi.org/10.1177/1534734620939748
30. Ganesh GV, Ramkumar KM: Macrophage mediation in normal and diabetic wound healing responses. Inflamm Res 2020; 69:347-363. https://doi.org/10.1007/s00011-020-01328-y
31. Jensen PO, Moller SA, Lerche CJ, Moser C, Bjarnsholt T, Ciofu O, Faurholt-Jepsen D et al: Improving antibiotic treatment of bacterial biofilm by hyperbaric oxygen therapy: Not just hot air. Biofilm 2019; 1:100008. https://doi.org/10.1016/j.bioflm.2019.100008